CHAPTER IV

CONTINUOUS STIRRED TANK REACTOR

A type of reactor used very commonly in industrial processing is a stirred tank operated continuously. It is referred to as the continuous stirred tank reactor (CSTR). One of the extensively investigated benchmarks for nonlinear control methodologies is the exothermic CSTR. The control of such processes requires a careful design because of their non-linearities and potentially unstable dynamics.

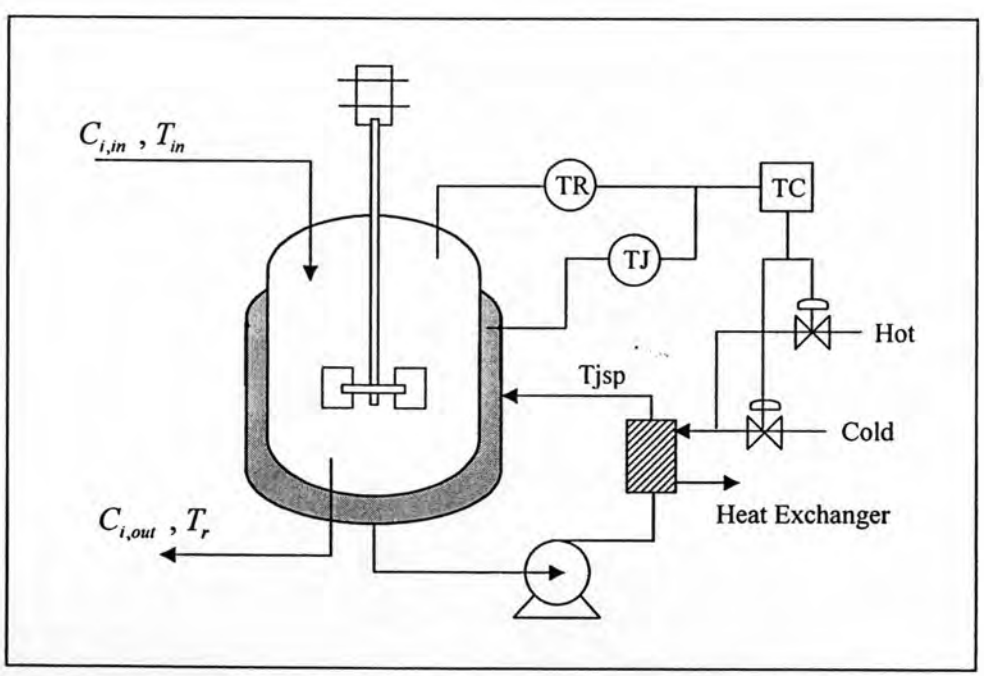

Figure 4.1 The schematic diagram of Continuous Stirred Tank Reactor

This chapter is divided into two sections: mathematical model and control study. In this work, a continuous stirred tank reactor (CSTR) developed by Perez and coworker (2002) is considered. The study is aimed at exothermic reaction for propylene glycol production (C) from propylene oxide (A) and water containing a small quantity of H_2SO_4 (B) and methanol (M). Methanol is added to prevent phase

splitting because propylene oxide is not completely soluble in water. A jacket is used to maintain the temperature of continuous stirred tank reactor (CSTR) as in set point. The schematic diagram of this system is shown in figure 4.1

4.1 Mathematical Model

The reaction for propylene glycol production (C) from propylene oxide (A) and water containing a small quantity of H_2SO_4 (B) and methanol (M) is carried out in CSTR can be represented as follows:

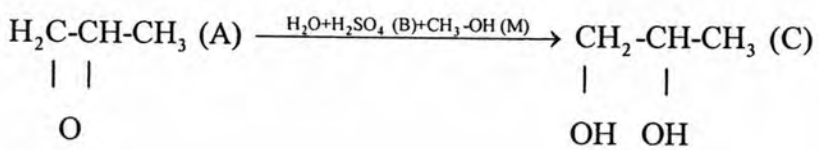

The assumptions are used in simulation as follows:

1. Concentration and temperature are distributed uniformly both in the reactor and the jacket.

2. The amount of heat retained in the reactor walls is negligible compared to the heat transferred in the reactor.

4.1.1 Material Balance

The components A, B, C, M mass balance are defined by the following equations;

$$\frac{dC_A}{dt} = \frac{q_{in}}{V}(C_{A,in} - C_A) - kC_A \tag{4.1}$$

$$\frac{dC_B}{dt} = \frac{q_{in}}{V}(C_{B,in} - C_B) - kC_A \tag{4.2}$$

$$\frac{dC_C}{dt} = \frac{q_{in}}{V}(-C_C) + kC_A \tag{4.3}$$

$$\frac{dC_M}{dt} = \frac{q_{in}}{V}(C_{M,in} - C_M) \tag{4.4}$$

$$k = \alpha e^{-E/RT} \tag{4.5}$$

Taking into account that the water is in excess, the reaction velocity of equations (4.1)–(4.3) is approximated by $-r_A = -r_B = r_C \approx kC_A$. The equation (4.5) is the Arrhenius law, $C_{A,in}$, $C_{B,in}$, $C_{C,in}$ and $C_{M,in}$ are the molar concentrations for the inlet stream, T is the reactor temperature, C_A, C_B, C_C and C_M are the molar concentrations for the outlet stream, q_{in} is the volumetric flow rate for the inlet stream, and V is the volume of the reactor. From the molar flow rates of A, B and M, the inlet volumetric flow rate q_{in} is determined by the equation:

$$q_{in} = \frac{F_{A,in}}{\rho_{A,in}} + \frac{F_{B,in}}{\rho_{B,in}} + \frac{F_{M,in}}{\rho_{M,in}} \tag{4.6}$$

where $F_{A,in}$, $F_{B,in}$, $F_{M,in}$ are the molar flow rates for the inlet stream and $\rho_{A,in}, \rho_{B,in}, \rho_{M,in}$ the molar densities of pure components A, B, M.

4.1.2 Energy Balance

The energy balance for the reactor can be written as

$$\frac{dT_r}{dt} = \frac{F_{A,in}C_{ps}(T_{in} - T_r) + Q_r - UA_j(T_r - T_j)}{VC_{pr}} \tag{4.7}$$

$$Q_r = (-\Delta H_r)kC_A V \tag{4.8}$$

where Q_r is the heat released from reaction, $-\Delta H_r$ is the enthalpy of reaction, U is the overall heat transfer coefficient of the jacket, A_j is the heat transfer area, T_j is the jacket temperature and T_{in} the inlet stream temperature. The parameter C_{ps} is defined by the equation:

$$C_{ps} = C_{pA} + \frac{F_{B,in}}{F_{A,in}}C_{pB} + \frac{F_{M,in}}{F_{A,in}}C_{pM} \tag{4.9}$$

where C_{pA} , C_{pB} , C_{pM} are the molar heat capacities for A, B, M respectively. The value of C_{pr} is calculated by the equation:

$$C_{pr} = C_{pA}C_A + C_{pB}C_B + C_{pC}C_C + C_{pM}C_M \tag{4.10}$$

where C_{pC} , C_C are the molar heat capacities and the concentration for the propylene glycol.

The energy balance for the jacket is

$$\frac{dT_j}{dt} = \frac{q_j}{V_j}(T_{jsp} - T_j) + \frac{UA_j}{\rho_j C_{pj} V_j}(T_r - T_j) \tag{4.11}$$

where q_j , ρ_j , C_{pj} are the volumetric flow rate, the density and the heat capacity of jacket respectively, V_j is the volume of the jacket , T_j is the jacket temperature and T_{jsp} is a set point value of the jacket temperature control system.

It is reasonable to assume that the dynamics of the jacket temperature control are approximately first order (Liptak, 1986) with time constant τ_j and, hence, the T_{jsp}, can be calculated by the following equation:

$$T_{jsp}(k) = T_j(k-1) + \frac{\tau_j(T_j(k) - T_j(k-1))}{dt} \tag{4.12}$$

where $\tau_j = V_j / q_j$

4.1.3 Nominal Operating Conditions

The operating conditions and parameter values for the nominal case simulation are given in table 4.1:

Table 4.1 The nominal operating conditions and parameter values

Variables	Values		Variables	Values	
A_j	33	m^2	$F_{B,in}$	7.712	kmol B/min
C_A	0.116	$kmol/m^3$	$F_{M,in}$	0.757	kmol M/min
C_B	36.256	$kmol/m^3$	q_{in}	0.1998	m^3/min
C_C	2.144	$kmol/m^3$	q_j	$2*q_{in}$	m^3/min
C_M	3.76	$kmol/m^3$	R	8.314	kJ/kmol K
$C_{A,in}$	2.26	$kmol/m^3$	U	355.4	kJ/min m^2 °C
$C_{B,in}$	38.4	$kmol/m^3$	V	14.16	m^3
$C_{M,in}$	3.76	$kmol/m^3$	V_j	1.416	m^3
C_{pA}	146.52	kJ/kg K	T_{in}	15.2	°C
C_{pB}	75.35	kJ/kg °C	α	$2.826x10^{11}$	min^{-1}
C_{pC}	192.57	kJ/kg °C	ρ_A	14.78	kmol A/m^3
C_{pM}	81.63	kJ/kg °C	ρ_B	55.27	kmol B/m^3
C_{pj}	4.18	kJ/kg °C	ρ_M	24.67	kmol M/m^3
E	75414	kJ/kmol	ρ_j	1000	kg/m^3
$F_{A,in}$	0.605	kmol A/min	ΔH	-83793	kJ/kmol

4.2 Control Study

The purpose of this study is to design the nonlinear adaptive control for a continuous stirred tank reactor to track the reactor temperature set point. A jacket is used to control the reactor temperature at its desired trajectory. Due to the heat-exchanger capacities, the jacket temperature is assumed to be limited to the range 25-120 °C.

For the simulation studies, equations (4.1)-(4.3) and (4.7)-(4.11) from the section 4.1 are solved to simulate the behavior of the reactor. The parameters and constant values used in the model are listed in Table 4.1.

4.2.1 Nonlinear Adaptive Control Configuration

A number of applications of adaptive control to the control of CSTR processes have been reported in many researches. However, most of these works the dynamic of jacket is not considered, but it is considered here. There are two approaches for constructing adaptive controllers. One is model-reference adaptive control method, and the other is self-tuning method. The later method, which is used in this research, is a controller that obtained by coupling a controller with an online parameter estimator. The controller that used in this method is generic model control (GMC); the controller parameter will be adjusted at any given period of time, coupled with the extended Kalman filter (EKF) to estimate the unknown parameter (heat released from reaction, Q_r).

4.2.1.1 Generic Model Control (GMC)

GMC is a model-based controller developed by Lee and Sullivan (1988). There are several advantages that make GMC a good control algorithm. The main advantage of the GMC is that the nonlinear process model does not need to be linearized because it directly inserts nonlinear process model into the controller itself.

The general form of the GMC control algorithm can be written as demonstrated in equation (3.8):

$$\frac{dy}{dt} = K_1(t)(y_{sp} - y) + K_2 \int (y_{sp} - y)dt$$

where y is the current value of controlled variable,

y_{sp} is a desired value of controlled variable,

K_1 and K_2 are tuning parameters of controller, which K_1 is adjustable parameter, and K_2 is constant.

The desired response can be obtained by incorporating two tuning parameters. The GMC defines the performance objective in terms of the time derivatives of the process output, i.e. minimizing the difference between the desired derivative of the process output and the actual derivative.

For temperature control of CSTR, the manipulated input of this tracking system is the jacket temperature, T_j and the tracked variable is the reactor temperature, T_r. It is assumed that the amount of heat retained in the walls of the reactor is small compared with the heat transferred in the reactor, an energy balance around the reactor contents gives in equation (4.7), as follow:

$$\frac{dT_r}{dt} = \frac{F_{A,in}C_{pr}(T_{in} - T_r) + Q_r - UA_j(T_r - T_j)}{VC_{pr}}$$

Substituting T_r for y and T_{rsp} for y_{rsp} in equation (3.8), combining equations (3.8) and (4.7), and finally solving for the manipulated variable, T_j, the control formulation is given by:

$$T_j = T_r - \frac{F_{A,in}C_{ps}}{UA_j}(T_{in} - T_r) - \frac{Q_r}{UA_j} + \frac{VC_{pr}}{UA_j}\left(K_1(T_{rsp} - T_r) + K_2 \int_0^t (T_{rsp} - T_r)dt \right)$$

(4.13)

The discrete form of equation (4.14) for the k^{th} time interval is given by:

$$T_j(k) = T_r(k) - \frac{F_{A,in}C_{ps}}{UA_j}\left(T_{in} - T_r(k)\right) - \frac{Q_r(k)}{UA_j}$$
$$+ \frac{VC_{pr}}{UA_j}\left(K_1(k)\left(T_{rsp} - T_r(k)\right) + K_2\sum_0^k \left(T_{rsp} - T_r(k)\right)dt \right) \qquad (4.14)$$

Considering the dynamics of T_j, if T_j is applied directly as the set point for jacket temperature control system, the result in control response would be sluggish. To accommodate such an effect, it is reasonable to assume that the dynamics of the jacket control system can be approximated by the first order model (Liptak, 1986), as follows:

$$T_{jsp}(k) = T_j(k-1) + \frac{\tau_j(T_j(k) - T_j(k-1))}{dt}$$

4.2.2.2 GMC with Extended Kalman Filter

As several model-based controllers, GMC requires the measurement or the estimation of the states of an appropriate process model. However, in most industrial, the state variables are not all measurable or, not with sufficient accuracy for control purposes. To succeed these difficulties, the estimation techniques have been used together with simplified process models. The flowchart of GMC with extended Kalman filter is shown in figure 4.2

As seen in equation (4.14), the success of the GMC controller is largely depended on the ability to measure, estimate, or predict the heat released, Q_r, at any given period of time. In this work, it is assumed that users have some knowledge. (perhaps, mistaken) of the physical parameters in the system: ΔH, C_{pr}, U, A_j. The extended Kalman filter is used to estimate Q_r by using the bilinear models (Kershenbaum and Kittisupakorn, 1994).

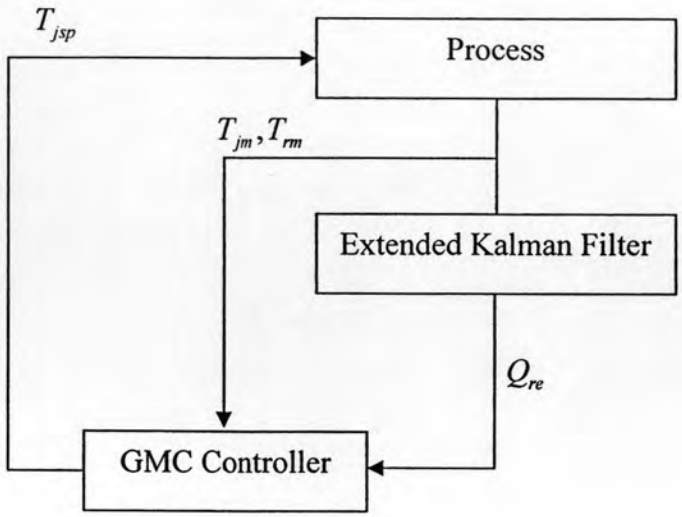

Figure 4.2 Flowchart of GMC with extended Kalman filter

A simple model, which attempts to reflect the basic chemical kinetics in the CSTR, is assumed that the rate of reaction, R, varies with respect to the reactant concentration, M_r, and the reactor temperature, T_{rm}, as shown in the following equations:

$$R = bM_r T_{rm} \tag{4.15}$$

where b is a pseudo reaction rate constant.

$$\frac{dM_r}{dt} = \frac{q_{in}(M_{r,in} - M_r)}{V} - R \tag{4.16}$$

The estimated heat released from the reaction is given by:

$$Q_r = (-\Delta H_r)VR = -bVM_r T_{rm} \Delta H_r \tag{4.17}$$

where ΔH_r is the heat of reaction

Define

$$N \equiv -bVM_r \Delta H_r \tag{4.18}$$

From energy balance on the reactor and jacket, the state equations for purposed of estimation are:

$$\frac{dT_{rm}}{dt} = \frac{F_{A,in}C_{pr}(T_{in} - T_{rm}) + Q_{re} - UA_j(T_{rm} - T_{jm})}{VC_{pr}} \tag{4.19}$$

$$\frac{dT_{jm}}{dt} = \frac{q_j}{V_j}(T_{jsp} - T_{jm}) + \frac{UA_j}{\rho_j C_{pj} V_j}(T_{rm} - T_{jm}) \tag{4.20}$$

$$\frac{dN}{dt} = -b\Delta H_r q_{in} M_{r,in} - \frac{Nq_{in}}{V} - bNT_{rm} \tag{4.21}$$

$$\frac{dQ_{re}}{dt} = N\frac{dT_{rm}}{dt} + T_{rm}\frac{dN}{dt} \tag{4.22}$$

$$\frac{db}{dt} = 0 \tag{4.23}$$

$$\frac{dUA_j}{dt} = 0 \tag{4.24}$$

T_{rm} and T_{jm} are measurable and are used to estimate the entire state, [T_{rm}, T_{jm}, N, Q_{re}, b, UA_j]^T, by an extended Kalman filter. The values of Kalman filter parameters and initial state estimates are given in Table 4.2.

Table 4.2 Klaman filter parameters and initial state estimates for simulation

T_r^0 = 54.2 °C	P(1,1) = 10^2	Q(1,1) = 3 x 10^3
T_j^0 = 53.6 °C	P(2,2) = 1	Q(2,2) = 1
N^0 = 553.2	P(3,3) = 10^3	Q(3,3) = 2 x 10^3
Q_{re}^0 = 3.59 x 10^4	P(4,4) = 10^3	Q(4,4) = 10^4
b^0 = 1.53 x 10^{-5}	P(5,5) = 10^3	Q(5,5) = 1
UA_j^0 = 1.17 x 10^4	P(6,6) = 10^6	Q(6,6) = 10^{10}
	R(1,1) = 0.1	R(2,2) = 0.1

4.2.2.3 Nonlinear Adaptive Controller

The nonlinear adaptive controller is a controller that obtained by coupling a nonlinear controller with an online parameter estimator. The operation of a nonlinear adaptive controller is as follows: at each time instant, the extended Kalman filter sends to the GMC controller the estimated heat released by reaction, Q_{re}, which is computed based on the output y, then finds the corresponding controller parameters, after that computes a control input u based on the controller parameters and measures signals; this control input u causes a new plant output to be generated, and the whole cycle of parameter and input updates is repeated.

From the control formulation in equation (4.14), the adjustable parameter is only K_1. So the corresponding controller parameter at the current time k can be calculated from the following equation:

$$K_1(k) = \frac{UA_j}{VC_{pr}} \frac{\left(T_j(k) - T_r(k)\right)}{\left(T_{rsp} - T_r(k)\right)} + \frac{1}{VC_{pr}} \frac{Q_{re}(k)}{\left(T_{rsp} - T_r(k)\right)} + \frac{F_{A,in}C_{ps}}{VC_{pr}} \frac{\left(T_{in} - T_r(k)\right)}{\left(T_{rsp} - T_r(k)\right)} - K_2 dt \frac{\left(2T_{rsp} - T_r(k) - T_r(k-1)\right)}{\left(T_{rsp} - T_r(k)\right)} \tag{4.25}$$

For K_1 at the previous time step $k-1$, the formulation is analogous to equation (4.25) as shown below:

$$K_1(k-1) = \frac{UA_j}{VC_{pr}} \frac{\left(T_j(k-1) - T_r(k-1)\right)}{\left(T_{rsp} - T_r(k-1)\right)} + \frac{1}{VC_{pr}} \frac{Q_{re}(k-1)}{\left(T_{rsp} - T_r(k-1)\right)} + \frac{F_{A,in}C_{ps}}{VC_{pr}} \frac{\left(T_{in} - T_r(k-1)\right)}{\left(T_{rsp} - T_r(k-1)\right)} - K_2 dt \frac{\left(2T_{rsp} - T_r(k-1) - T_r(k-2)\right)}{\left(T_{rsp} - T_r(k-1)\right)} \tag{4.26}$$

Hence, the relationship between K_1 at the current time step (k) and the previous time step $(k-1)$ as shown below:

$$K_1(k) = K_1(k-1) + \frac{UA_j}{VC_{pr}}\left(\frac{T_j(k)}{\left(T_{rsp} - T_r(k)\right)} - \frac{T_j(k-1)}{\left(T_{rsp} - T_r(k-1)\right)}\right)$$
$$+ \frac{1}{VC_{pr}}\left(\frac{Q_{re}(k)}{\left(T_{rsp} - T_r(k)\right)} - \frac{Q_{re}(k-1)}{\left(T_{rsp} - T_r(k-1)\right)}\right) + \frac{\left(T_r(k) - T_r(k-1)\right)W_1 + W_2}{\left(T_{rsp} - T_r(k)\right)\left(T_{rsp} - T_r(k-1)\right)} \quad (4.27)$$

where W_1 and W_2 are given by:

$$W_1 = -T_{rsp}\left(\frac{UA_j}{VC_{pr}} + \frac{F_{A,in}C_{ps}}{VC_{pr}} + 2K_2 dt\right) + \frac{F_{A,in}C_{ps}}{VC_{pr}}T_{in} \quad (4.28)$$

$$W_2 = K_2 dt\left(T_{rsp}\left(T_r(k) - T_r(k-2)\right) - Tr^2(k-1) + Tr(k)Tr(k-2)\right) \quad (4.29)$$

K_1 is bounded between -30% and +30% of initial value. The value of K_1 at current time is set to be equal to K_1 at previous time step when the absolute error between the reactor temperature and the temperature set point is less than 1.

The diagram of nonlinear adaptive controller is shown in figure 4.3

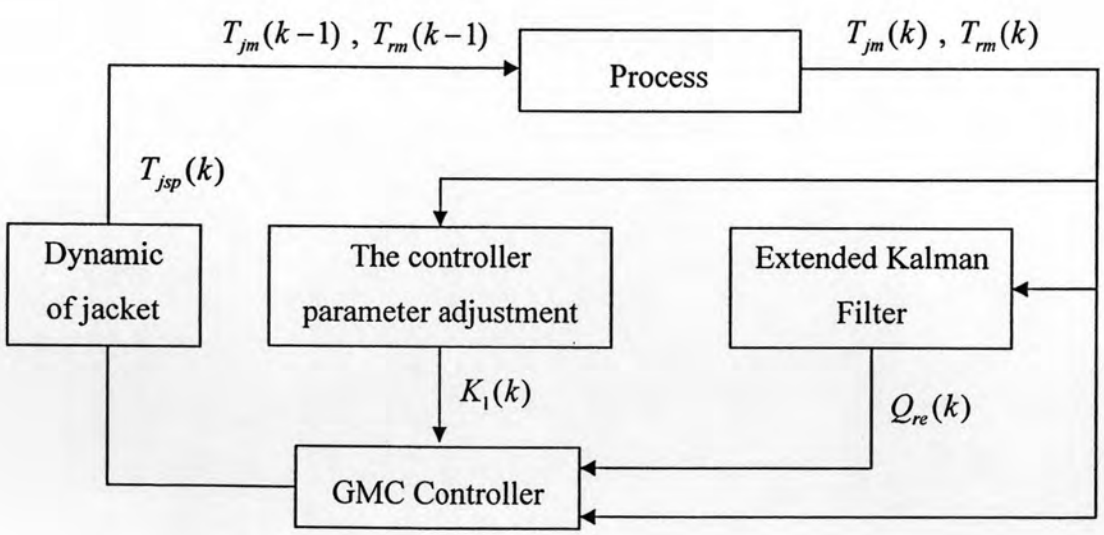

Figure 4.3 The diagram of nonlinear adaptive controller

4.2.2 Control Results and Discussion

This section demonstrates the simulation studies which are carried out to investigate the performance of nonlinear adaptive control, which use GMC as a controller coupled with EKF to estimate heat released by reaction. The objective is to control the reactor temperature set point at 54.2 °C. That the control manipulated input, represents the jacket temperature while the controlled output is the reactor temperature. The control results of nonlinear adaptive controller are also compared with the performance of GMC and conventional PID controller in cases of disturbance rejection, in which all model parameter used to simulate are specified correctly, and plant/model mismatches, in which some parameters have changed from their nominal values. Moreover, the Integral of Absolute Error (IAE) is utilized as the control performance indices. We assume that the CSTR is initially controlled at its nominal steady state value until all changes of disturbance, which is inlet volumetric flow rate (q_{in}), and mismatch are introduced to the system at the t = 20 min and kept throughout the simulation. At this point, the controller is still set at its initial value until at t = 150 min the controller is then activated.

In this research, the appropriate value of the tuning parameters of nonlinear adaptive, GMC and conventional PID controller that used for all simulations are given in Table 4.3. Two measurements (T_r and T_j) are available and are used to obtain estimates of the entire state, $[T_{rm}, T_{jm}, N, Q_{re}, b, UA_j]^T$, using an extended Kalman filter. The values of Kalman filter parameters and initial state estimates are given in Table 4.2.

Table 4.3 The tuning parameters of controllers

Controller	**Tuning parameters**		
Nonlinear adaptive	$K_1^0 = 5.0129$	$K_2 = 3.916\text{x}10^{-3}$	
GMC	$K_1 = 5.0129$	$K_2 = 3.916\text{x}10^{-3}$	
PID	$K_c = 325$	$\tau_i = 2.484$	$\tau_d = 0.22$

The robustness test is divided into two cases:

- Model-Mismatch

In this case, the mismatch caused by model of the controller has no effect to conventional PID controller, because the PID controller is not a model-based controller. Therefore, it will have an effect to nonlinear adaptive control and GMC controller. In this case, the robustness test is divided into two cases:

  - Increase 20% of overall heat transfer, U
  - Decreases 20% of overall heat transfer, U

- Plant-Mismatch

In this case, the mismatch caused by process change has an effect to nonlinear adaptive, GMC and PID controller. The robustness test divided into six cases:

  - Increase 20% of overall heat transfer, U
  - Decreases 20% of overall heat transfer, U
  - Increase 20% of heat of reaction, ΔH_r
  - Decrease 20% of heat of reaction, ΔH_r
  - Increase 20% of rate constant, k
  - Decrease 20% of rate constant, k

Case 1: Nominal case

The inlet volumetric flow rate, q_{in}, is increased 30% from the nominal operating condition. The simulation results for nonlinear adaptive, GMC and PID controller are shown in figure 4.4-4.5. The IAE values are 387.01, 387.01 and 387.01 for nonlinear adaptive, GMC and PID, respectively.

Figure 4.4(a) shows the response of nonlinear adaptive controller to track the reactor temperature set point. The performance of EKF to estimate the heat released by reaction can be seen in figure 4.5(a). It provides excellent estimation of the heat released. For the controller parameter adjustment is illustrated in figure 4.5(b). With this heat released and parameter adjustment, the nonlinear adaptive controller gives very good control performance without overshoot in this case. In comparison, figure 4.4 shows that the nonlinear adaptive control, GMC and PID controller give the same response. Due to in this case, tuning parameter of the controllers are tuned to achieve the same values of IAE.

Case 2: Model-Mismatches

- Increase 20% of overall heat transfer, *U*

The overall heat transfer, *U*, in model of controller is increased 20% from the nominal operating condition. The simulation results for nonlinear adaptive and GMC controller are shown in figure 4.6-4.7. The IAE values are 387.73 and 388.08 for nonlinear adaptive and GMC, respectively.

- Decreased 20% of overall heat transfer, *U*

The overall heat transfer, *U*, in model of controller is decreased 20% from the nominal operating condition. The simulation results for nonlinear adaptive and GMC controller are shown in figure 4.8-4.9. The IAE values are 387.76 and 387.99 for nonlinear adaptive and GMC, respectively.

In this mismatch cases, the nonlinear adaptive control shows quite good control performance as shown in figure 4.6(a) and 4.8(a). Furthermore, the EKF is able to estimate the heat released by reaction close to the true value as illustrated in figure 4.7(a) and 4.9(a). Figure 4.7(b) and 4.9(b) show the controller parameter adjustment. The comparison of control response between the nonlinear adaptive control and GMC in figure 4.6 and 4.8 shows that the response of the nonlinear adaptive control as same as GMC in both cases.

Case 3: Plant-Mismatches

- Increase 20% of overall heat transfer, *U*

The overall heat transfer, *U*, in plant model is increased 20% from the nominal operating condition. The simulation results for nonlinear adaptive, GMC and PID controller are shown in figure 4.10-4.11. The IAE values are 367.99, 368.21 and 368.24 for nonlinear adaptive, GMC and PID, respectively.

- Decreases 20% of overall heat transfer, *U*

The overall heat transfer, *U*, in plant model is decreased 20% from the nominal operating condition. The simulation results for nonlinear adaptive, GMC and PID controller are shown in figure 4.12-4.13. The IAE values are 416.51, 416.79 and 416.86 for nonlinear adaptive, GMC and PID, respectively.

When the overall heat transfer in plant model is changed, the nonlinear adaptive controller has still provided good control performance in both cases as shown in figure 4.10(a) and 4.12(a). Figure 4.11(a) and 4.13(a) present the performance of the EKF for estimates the heat released when the overall heat transfer increased and decreased 20%, respectively. Since the EKF estimates the heat released by reaction close to the true value, the mismatch is eliminated. The controller parameter adjustment is shown in figure 4.11(b) and 4.13(b).

The performance of the nonlinear adaptive control for increasing 20% of overall heat transfer compared with GMC and PID is shown in Figure 4.10. It can be found that the nonlinear adaptive gives control response as same as GMC, but faster than the response of PID. Figure 4.12 shows that the performance of the nonlinear adaptive control when overall heat transfer is decreased 20% as same as GMC, but better than the performance of PID. The control action of PID is more overshooting response.

- Increase 20% of heat of reaction, ΔH_r

The heat of reaction, ΔH_r, in plant model is increased 20% from the nominal operating condition. The simulation results for nonlinear adaptive, GMC and PID controller are shown in figure 4.14-4.15. The IAE values are 859.21, 859.34 and 876.80 for nonlinear adaptive, GMC and PID, respectively.

- Decrease 20% of heat of reaction, ΔH_r

The heat of reaction, ΔH_r, in plant model is decreased 20% from the nominal operating condition. The simulation results for nonlinear adaptive, GMC and PID controller are shown in figure 4.16-4.17. The IAE values are 59.36, 59.37 and 60.01 for nonlinear adaptive, GMC and PID, respectively.

From figure 4.15(a) and 4.17(a), it can be seen that heat released by reaction and the reactor temperature are sensitive to changing heat of reaction. Heat released by reaction and the reactor temperature increase when heat of reaction is increased. On the other hand, heat released and the reactor temperature decrease when heat of reaction is decreased. The EKF gives a reasonable estimation in both cases. In case of increasing heat of reaction, the nonlinear adaptive control is found that it provides good control performance as same as GMC, but better than the performance of PID. The PID controller provides overshoot response. The control responses are shown in figure 4.14. The response of the nonlinear adaptive control is faster control action than PID when the heat of reaction is decreased 20% from the nominal condition as shown in figure 4.16. For the controller parameter adjustment is illustrated in figure 4.15(b) and 4.17(b).

- Increase 20% of rate constant, *k*

The rate constant, *k*, in plant model is increased 20% from the nominal operating condition. The simulation results for nonlinear adaptive, GMC and PID controller are shown in figure 4.18-4.19. The IAE values are 415.45, 415.50 and 415.82 for nonlinear adaptive, GMC and PID, respectively.

- Decrease 20% of rate constant, *k*

The rate constant, *k*, in plant model is decreased 20% from the nominal operating condition. The simulation results for nonlinear adaptive, GMC and PID controller are shown in figure 4.20-4.21. The IAE values are 346.56, 346.60 and 347.09 for nonlinear adaptive, GMC and PID, respectively.

In case of the rate constant changes, it can be found that the nonlinear adaptive controller is still robust as shown in figure 4.18(a) and 4.20(a). For estimation, the EKF gives good estimation of heat released by reaction as shown in figure 4.19(a) and 4.21(a). The controller parameter adjustment can be seen in figure 4.19(b) and 4.21(b). When the rate constant is increased 20%, the nonlinear adaptive control gives control performance as same as GMC, but better than the performance of PID controller. The control action of PID is more overshooting response as demonstrated in figure 4.18. In case of decreasing of rate constant, the response of the nonlinear adaptive control is faster control action than PID controller as shown in figure 4.21.

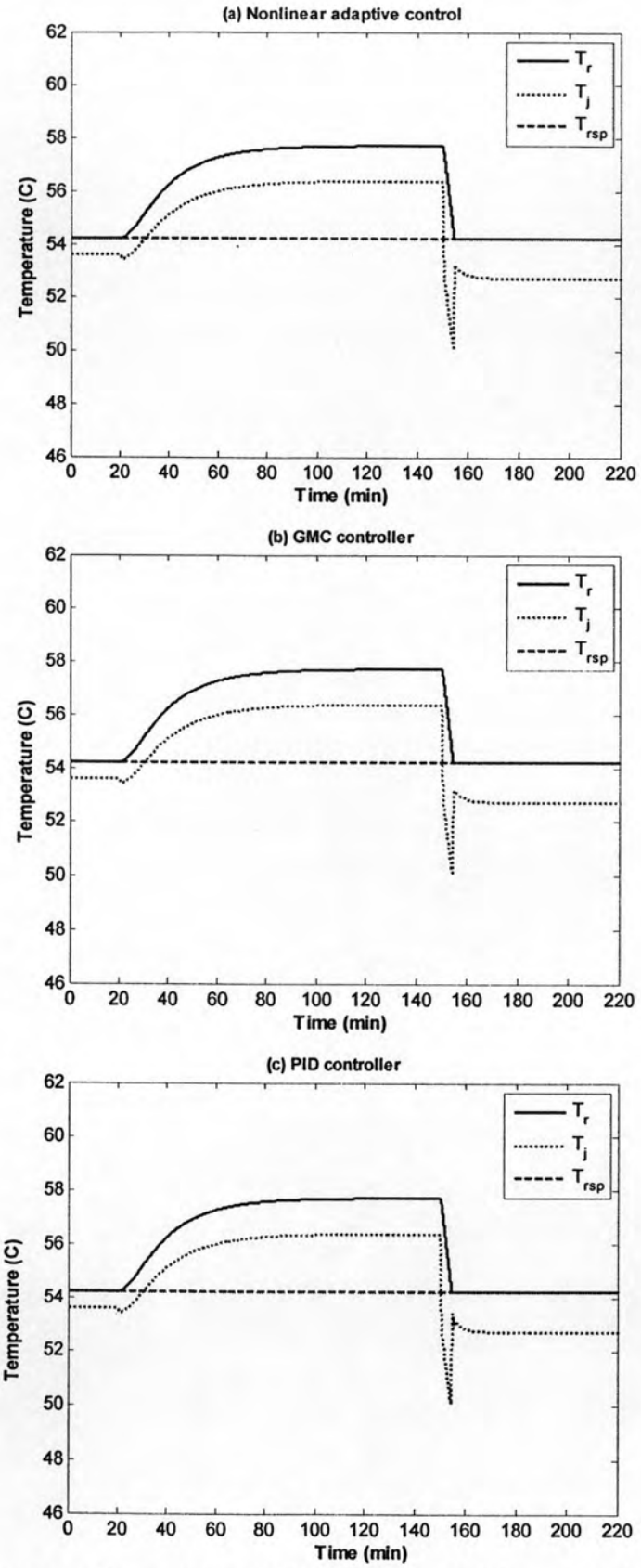

Figure 4.4 The control response of (a) nonlinear adaptive control (b) GMC and (c) PID in nominal case

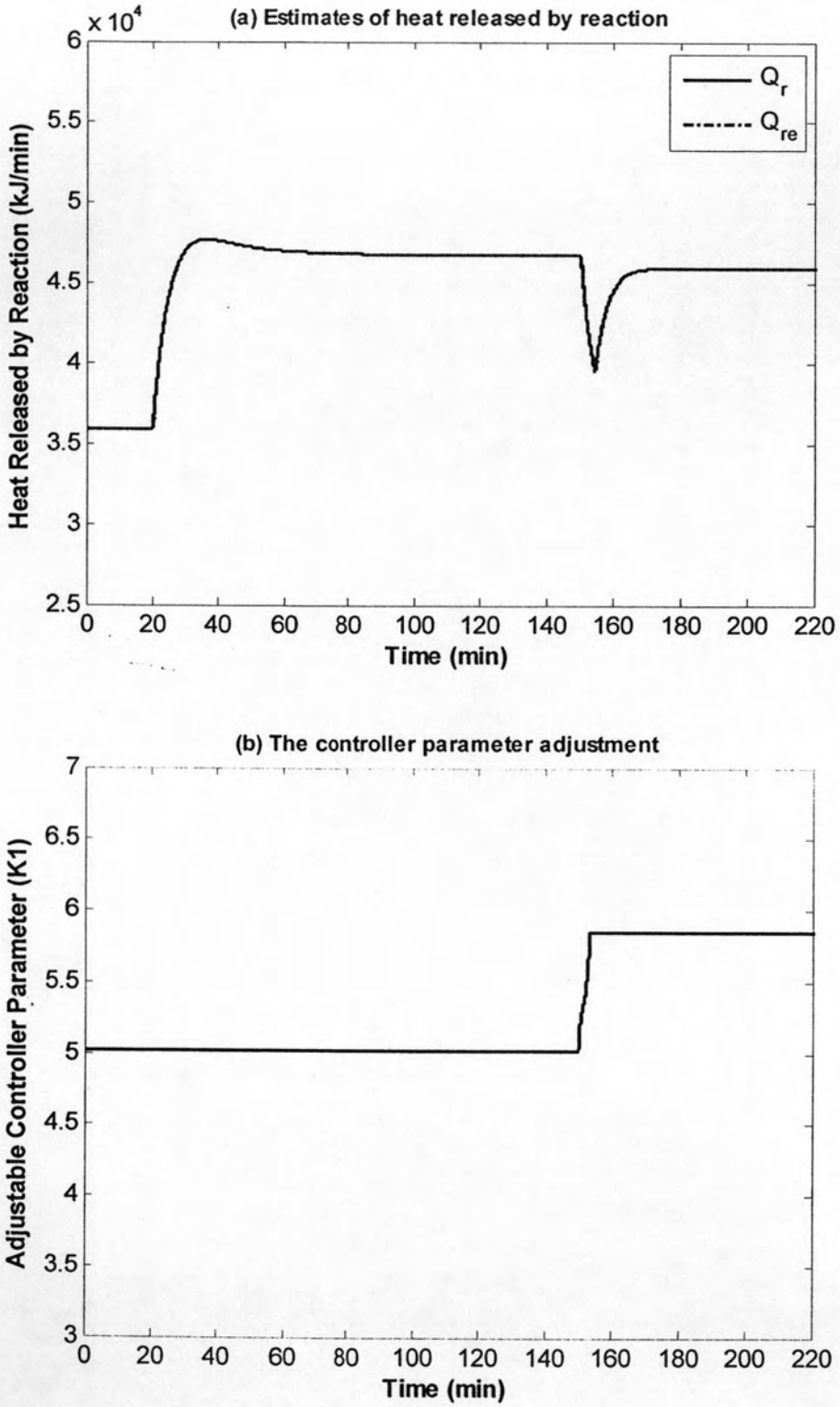

Figure 4.5 (a) Estimates of heat released by reaction and (b) the controller parameter adjustment in nominal case

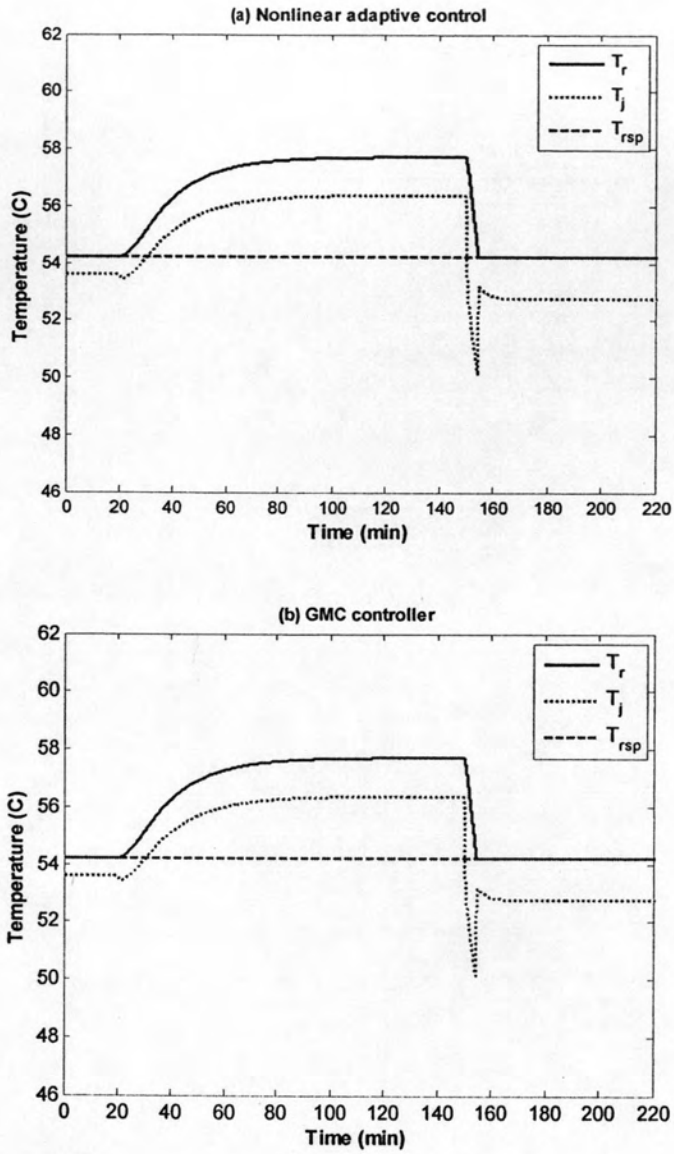

Figure 4.6 The control response of (a) nonlinear adaptive control and (b) GMC in model-mismatch case, +20% U

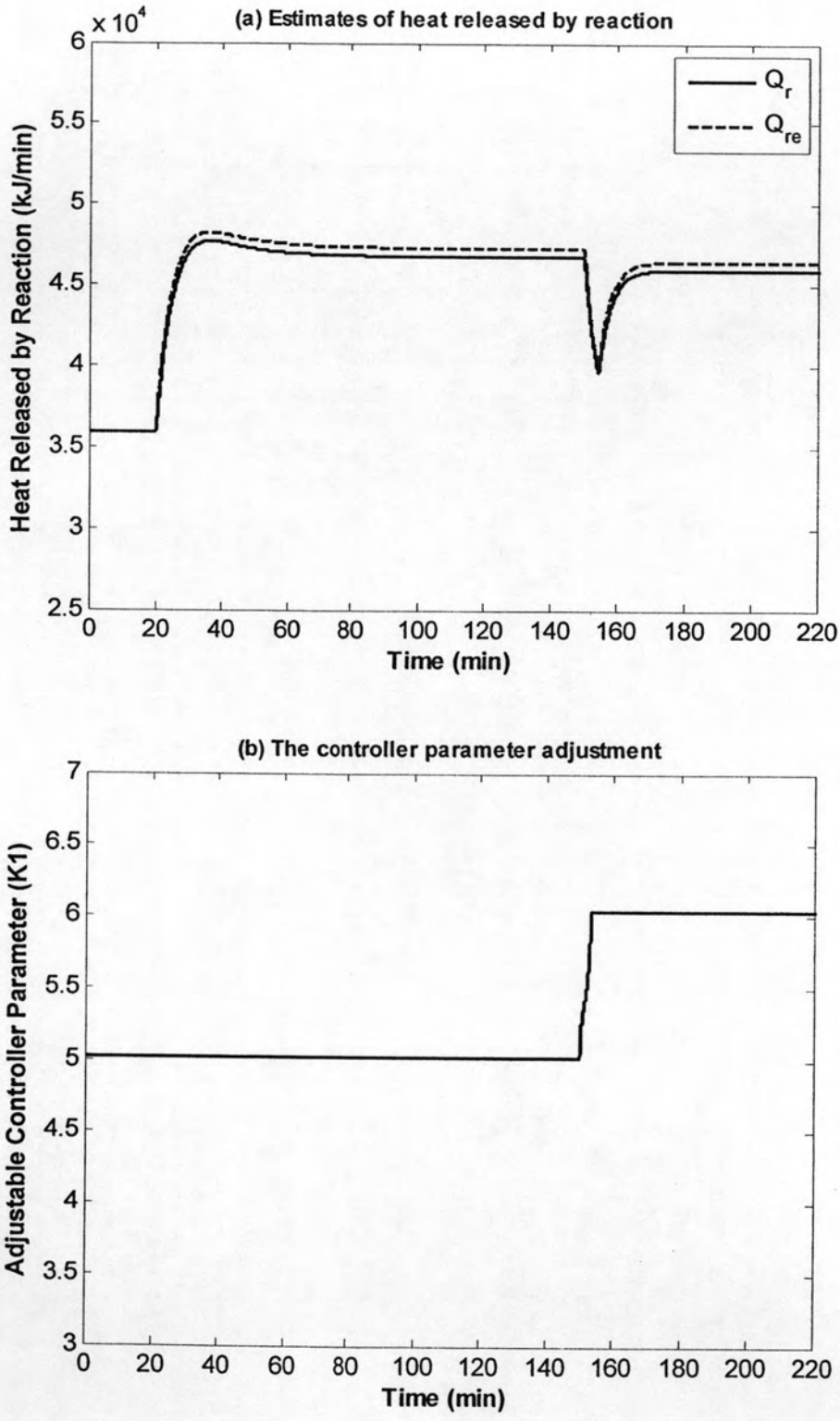

Figure 4.7 (a) Estimates of heat released by reaction and (b) the controller parameter adjustment in model-mismatch case, +20% U

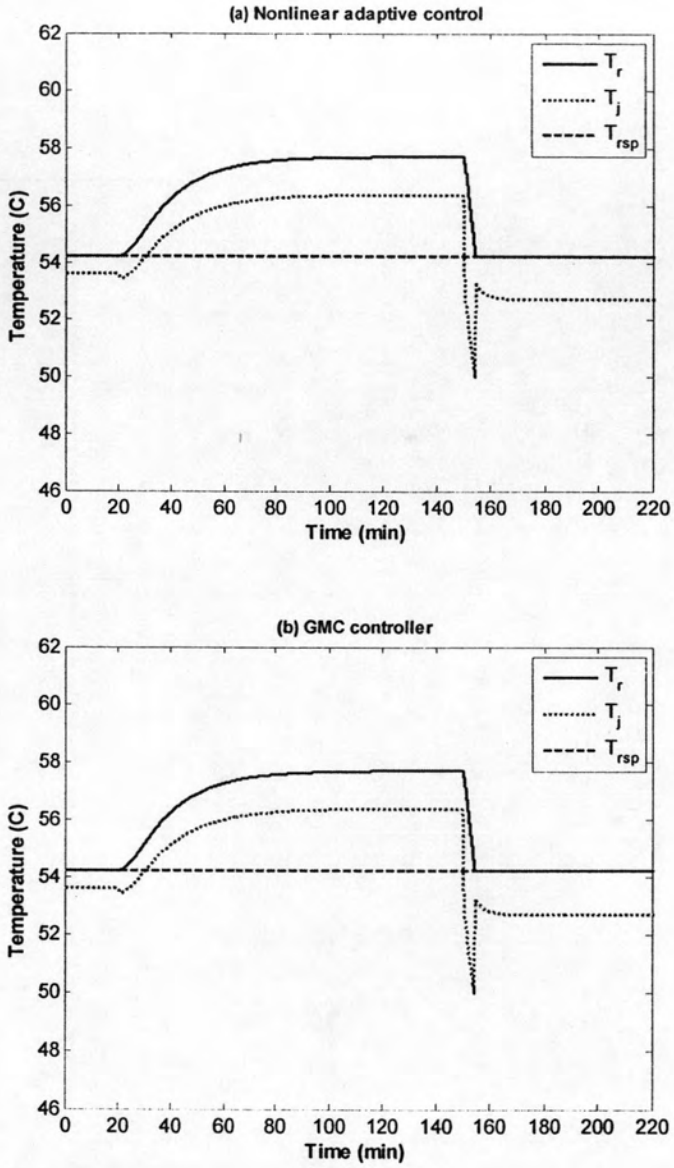

Figure 4.8 The control response of (a) nonlinear adaptive control and (b) GMC in model-mismatch case, -20% U

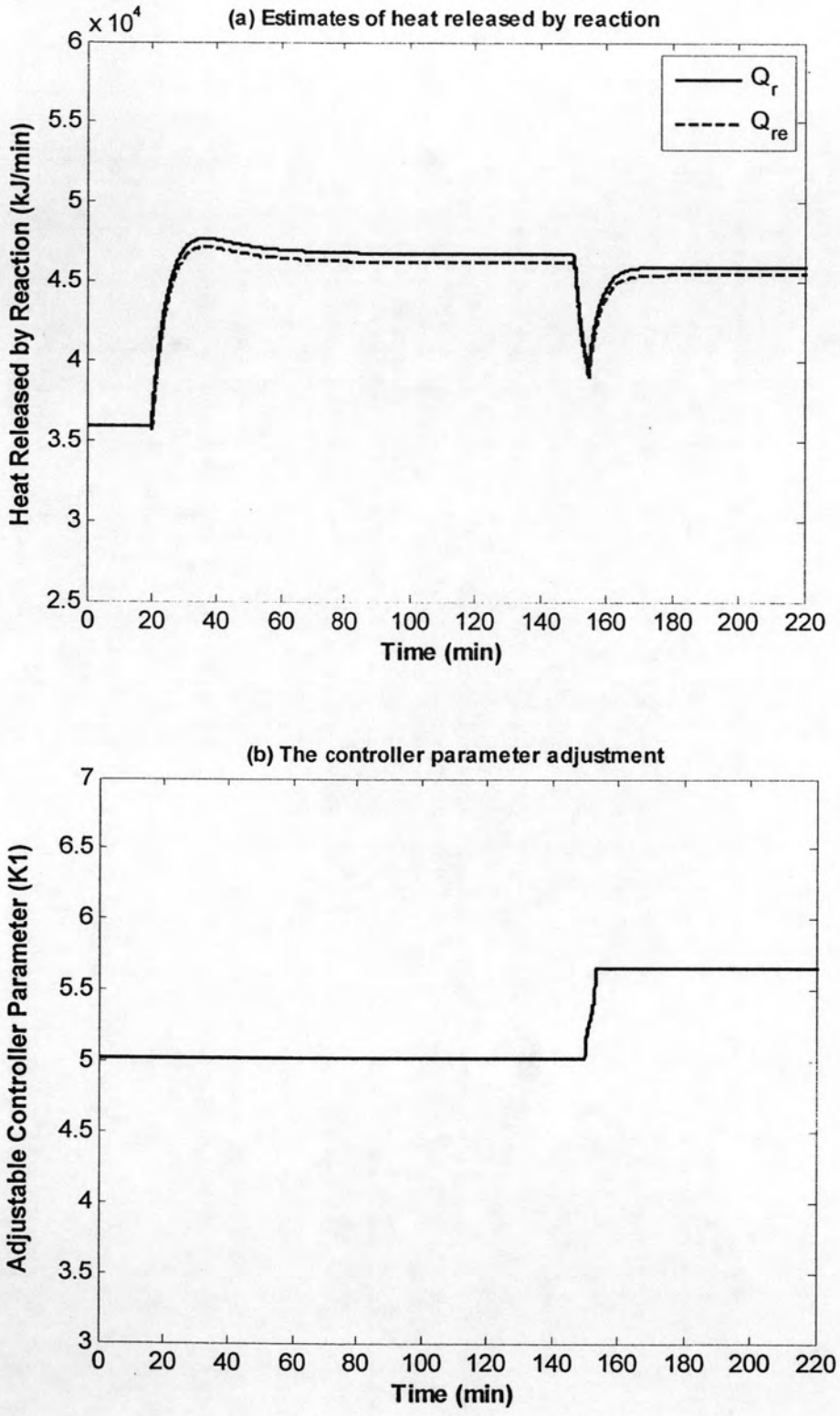

Figure 4.9 (a) Estimates of heat released by reaction and (b) the controller parameter adjustment in model-mismatch case, -20% *U*

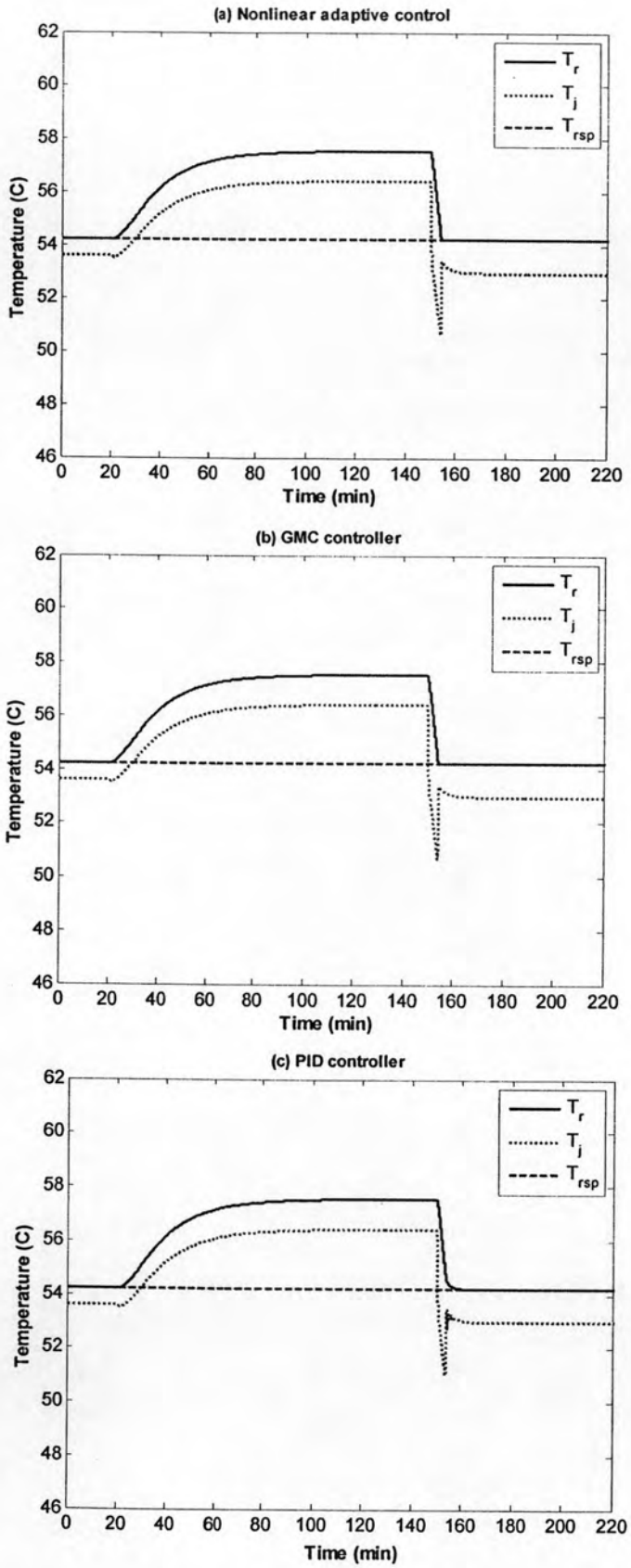

Figure 4.10 The control response of (a) nonlinear adaptive control (b) GMC and (c) PID in plant-mismatch case, +20% *U*

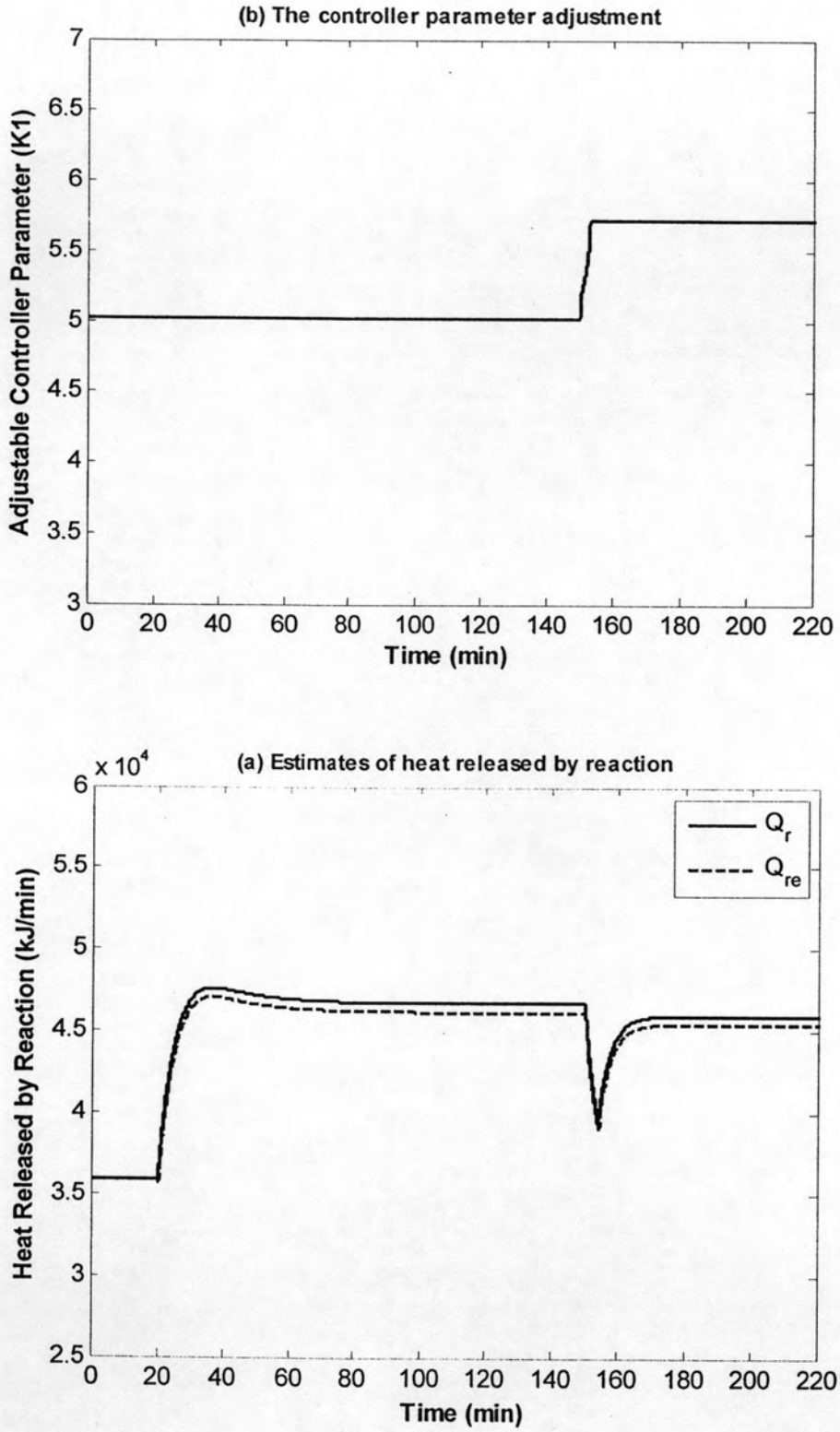

Figure 4.11 (a) Estimates of heat released by reaction and (b) the controller parameter adjustment in plant-mismatch case, +20% U

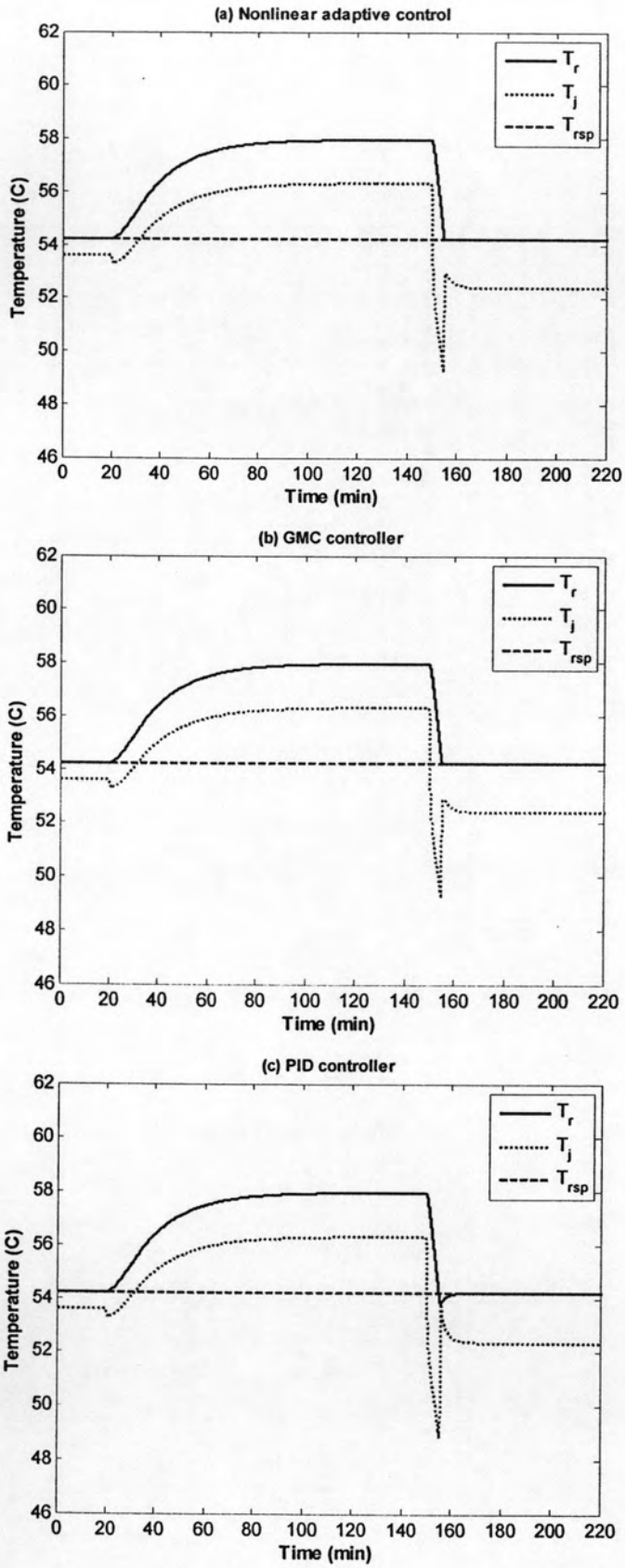

Figure 4.12 The control response of (a) nonlinear adaptive control (b) GMC and (c) PID in plant-mismatch case, -20% *U*

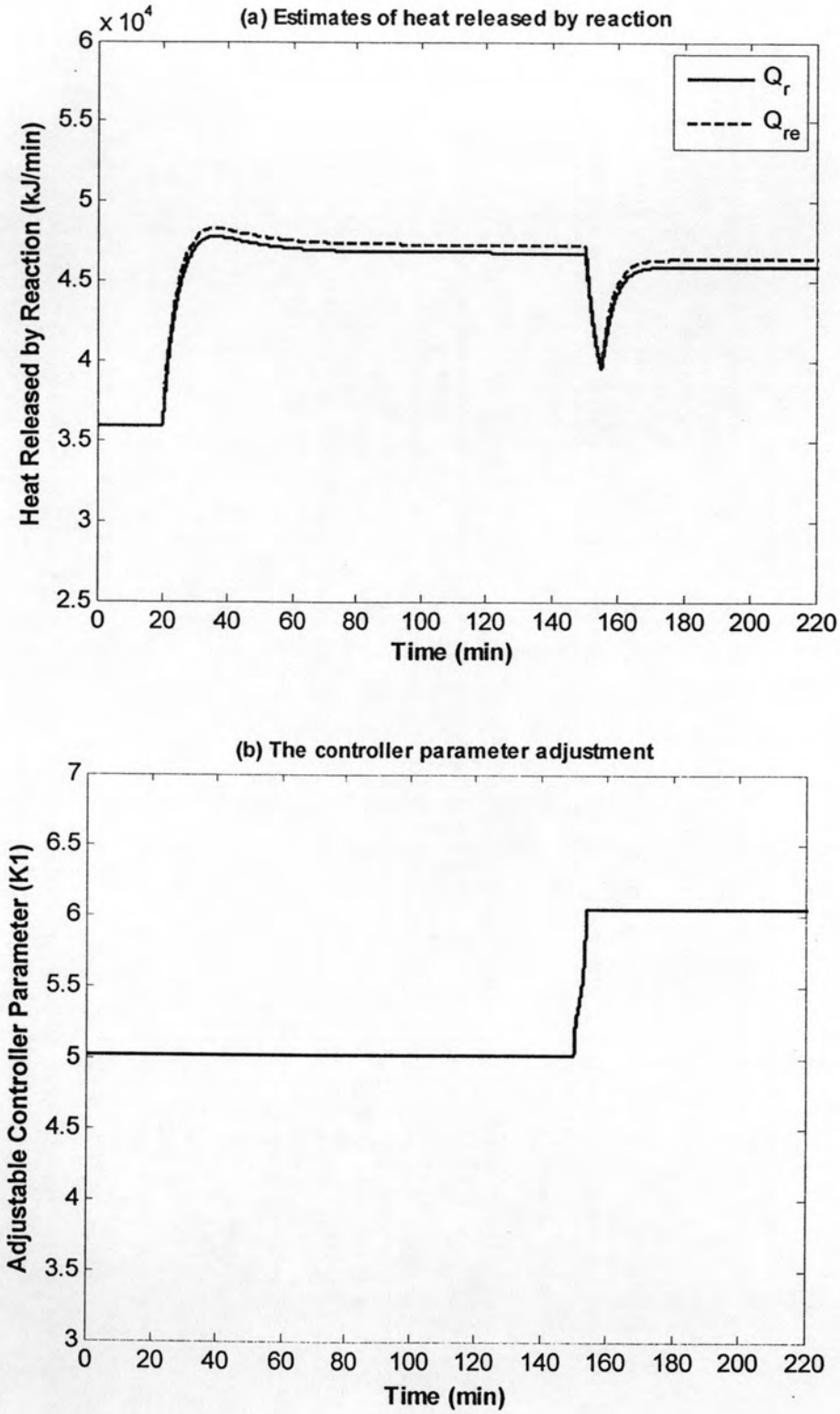

Figure 4.13 (a) Estimates of heat released by reaction and (b) the controller parameter adjustment in plant-mismatch case, -20% *U*

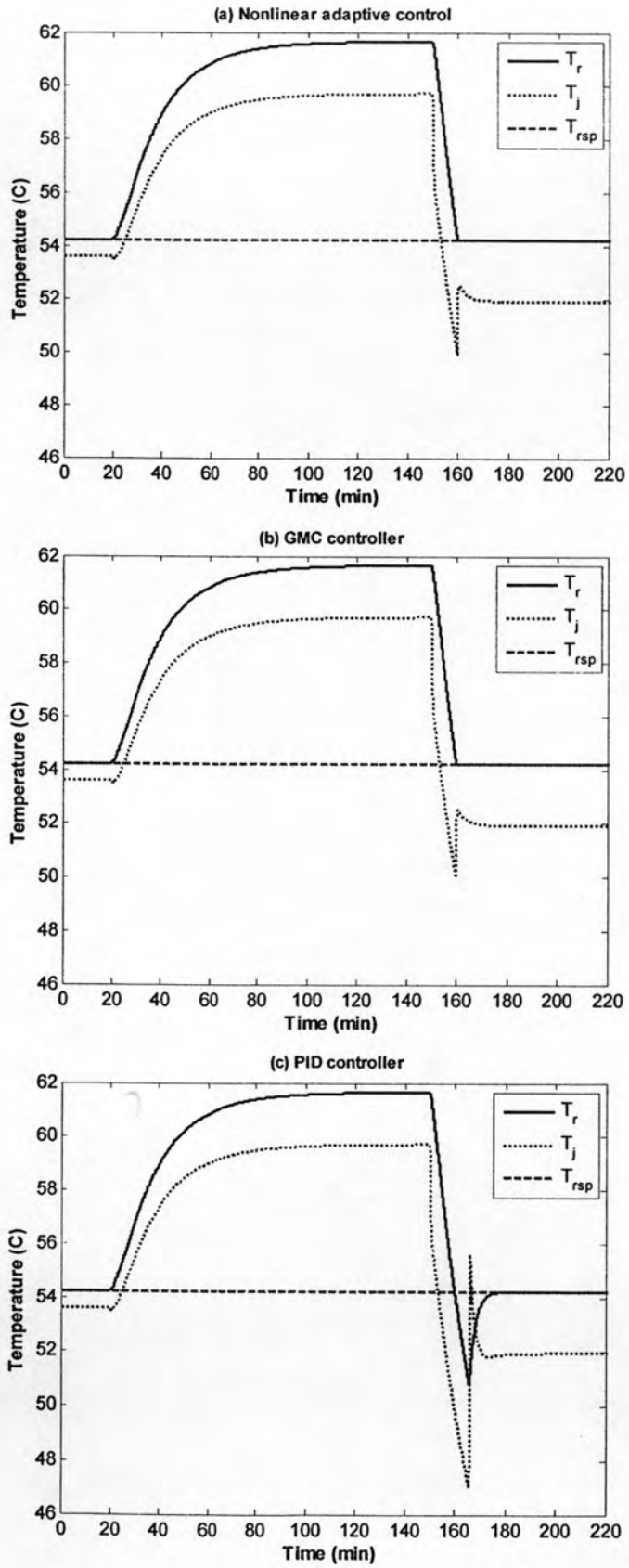

Figure 4.14 The control response of (a) nonlinear adaptive control (b) GMC and (c) PID in plant-mismatch case, +20% ΔH_r

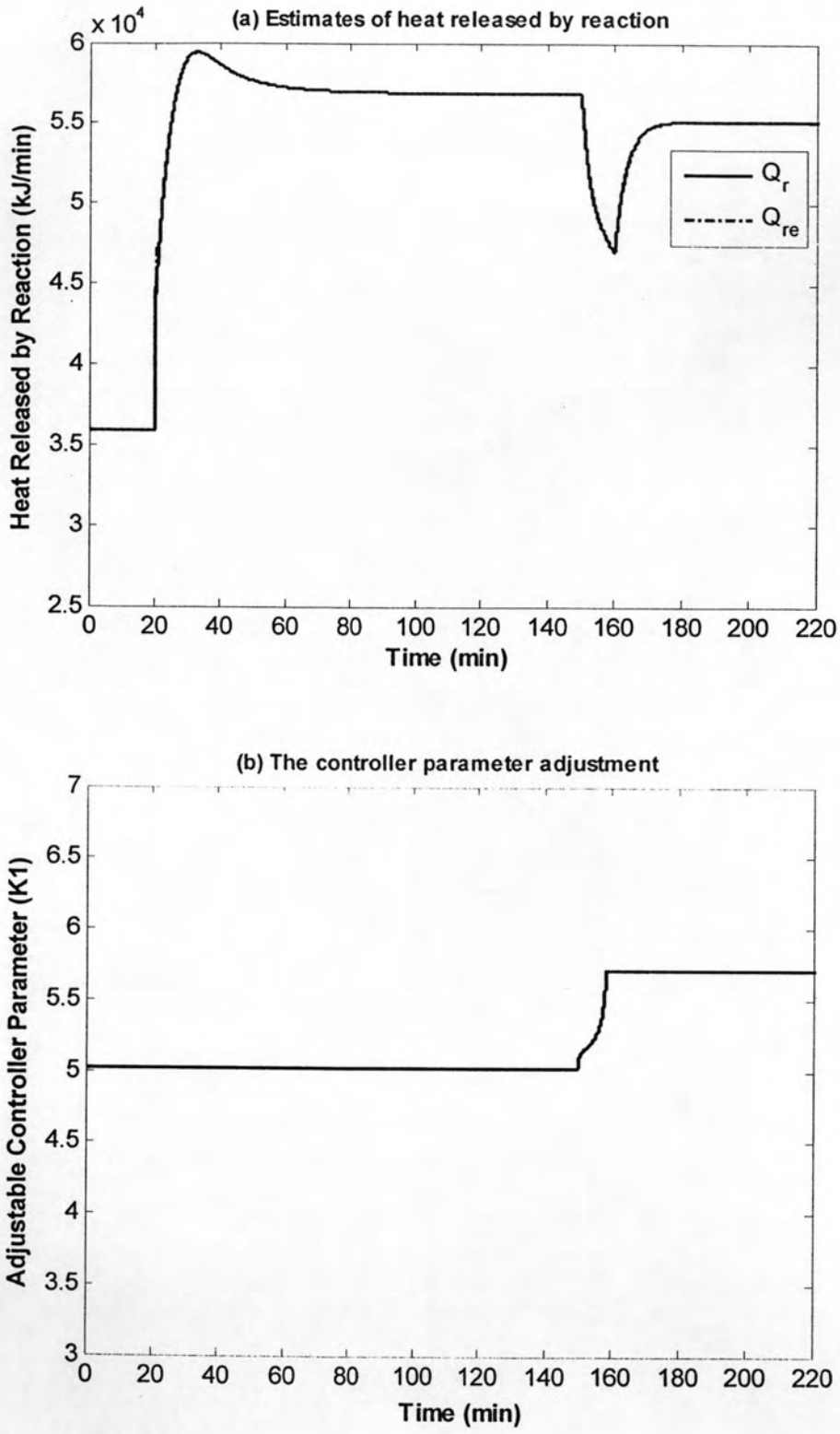

Figure 4.15 (a) Estimates of heat released by reaction and (b) the controller parameter adjustment in plant-mismatch case, +20% ΔH_r

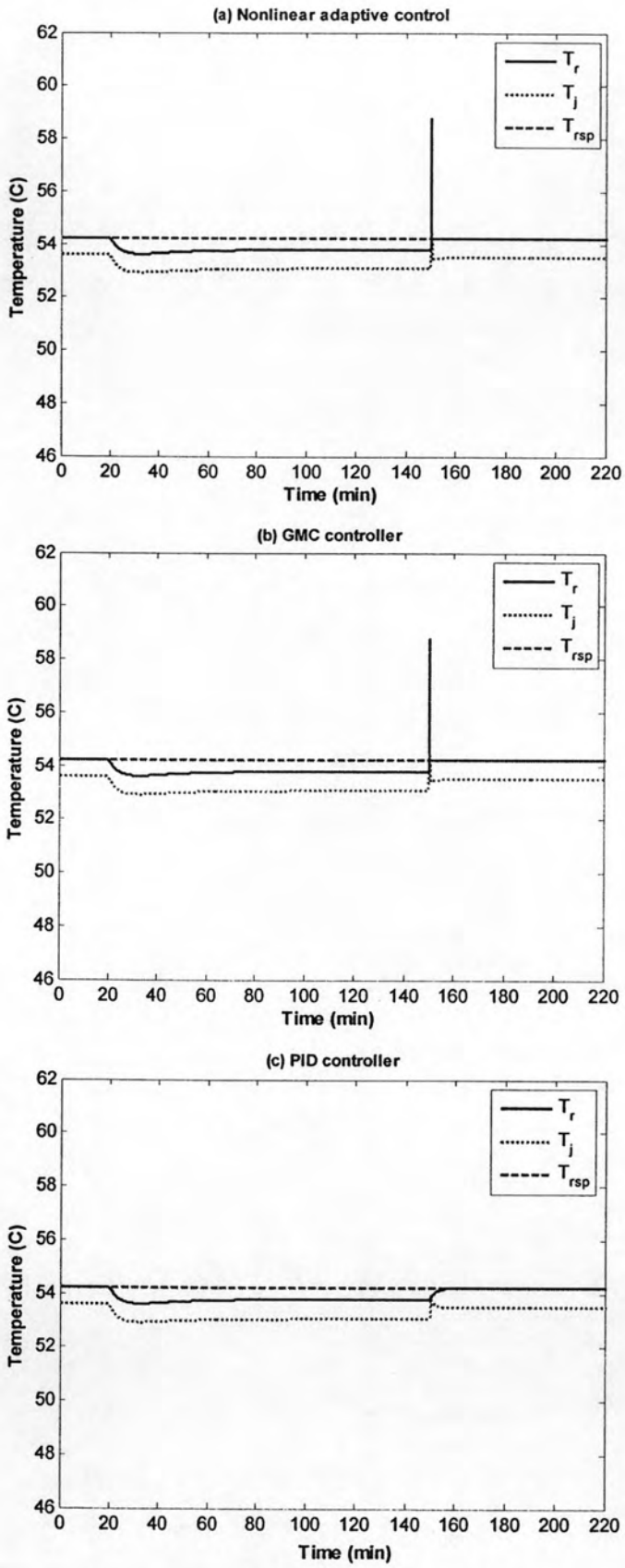

Figure 4.16 The control response of (a) nonlinear adaptive control (b) GMC and (c) PID in plant-mismatch case, -20% ΔH_r

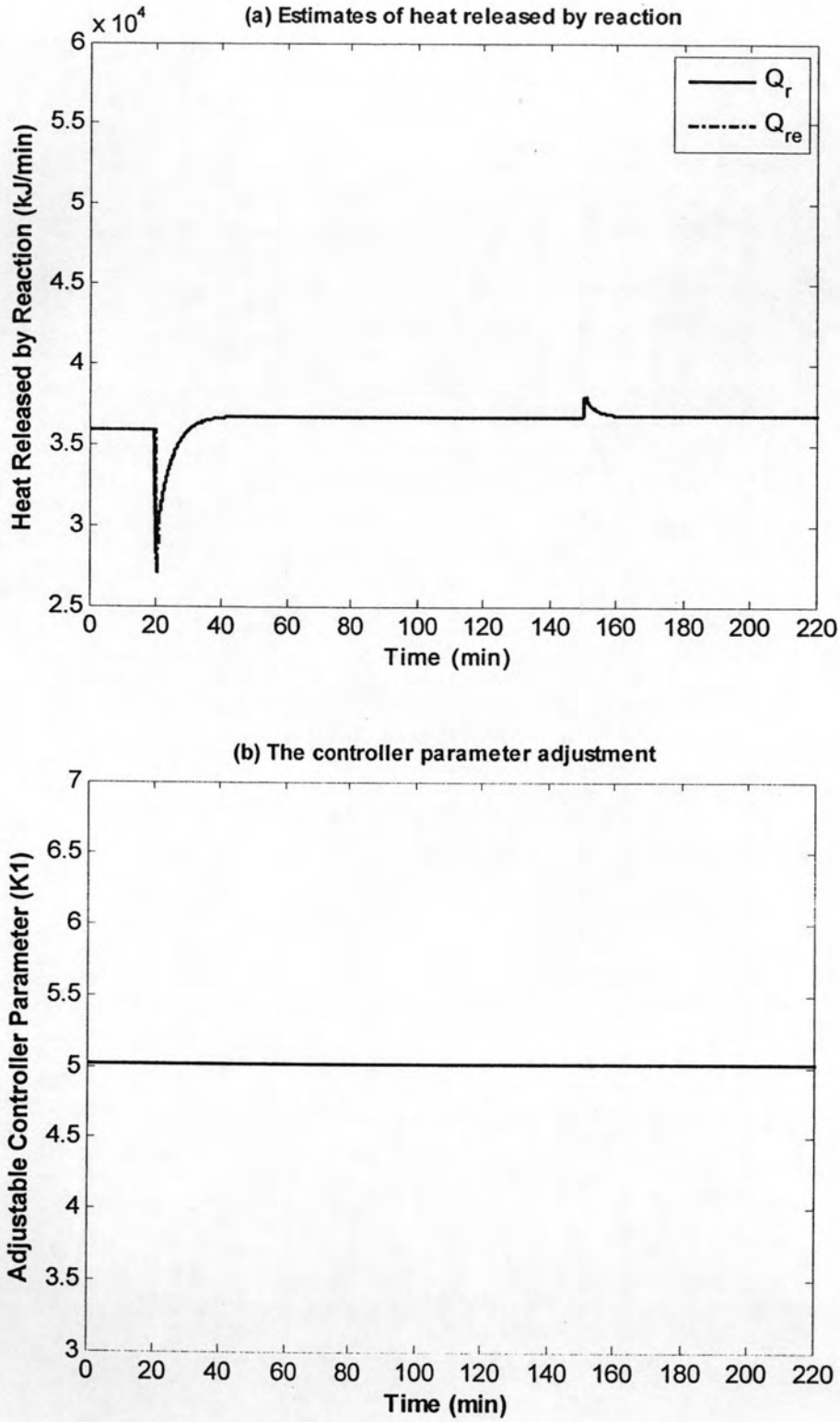

Figure 4.17 (a) Estimates of heat released by reaction and (b) the controller parameter adjustment in plant-mismatch case, -20% ΔH_r

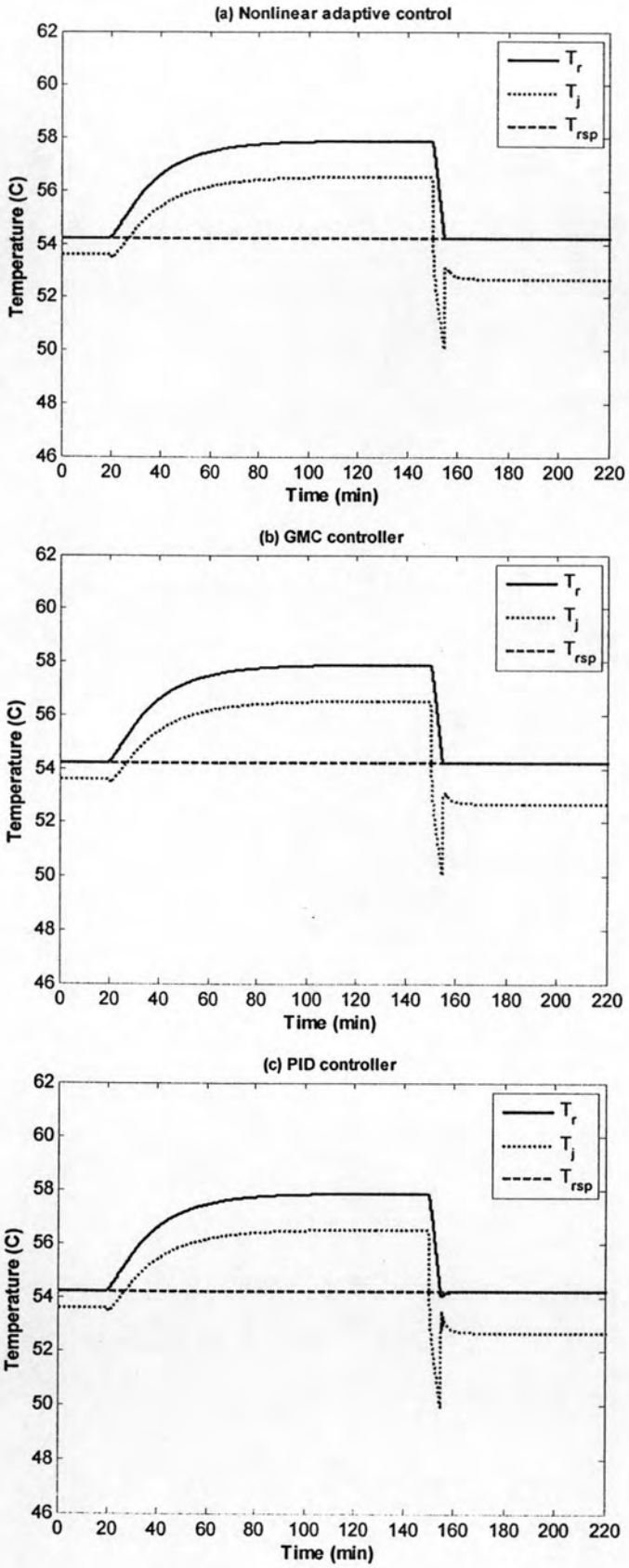

Figure 4.18 The control response of (a) nonlinear adaptive control (b) GMC and (c) PID in plant-mismatch case, +20% k

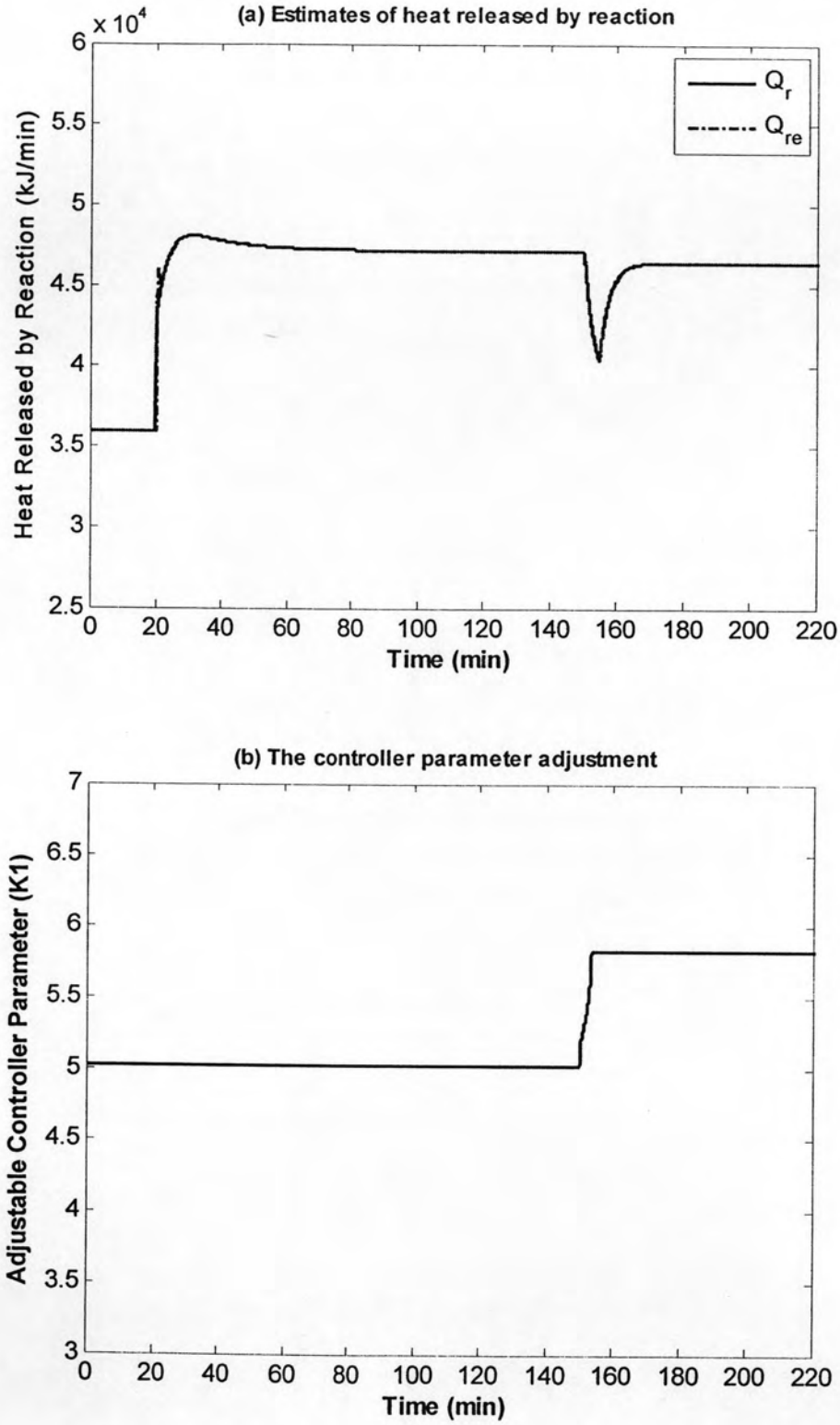

Figure 4.19 (a) Estimates of heat released by reaction and (b) the controller parameter adjustment in plant-mismatch case, +20% k

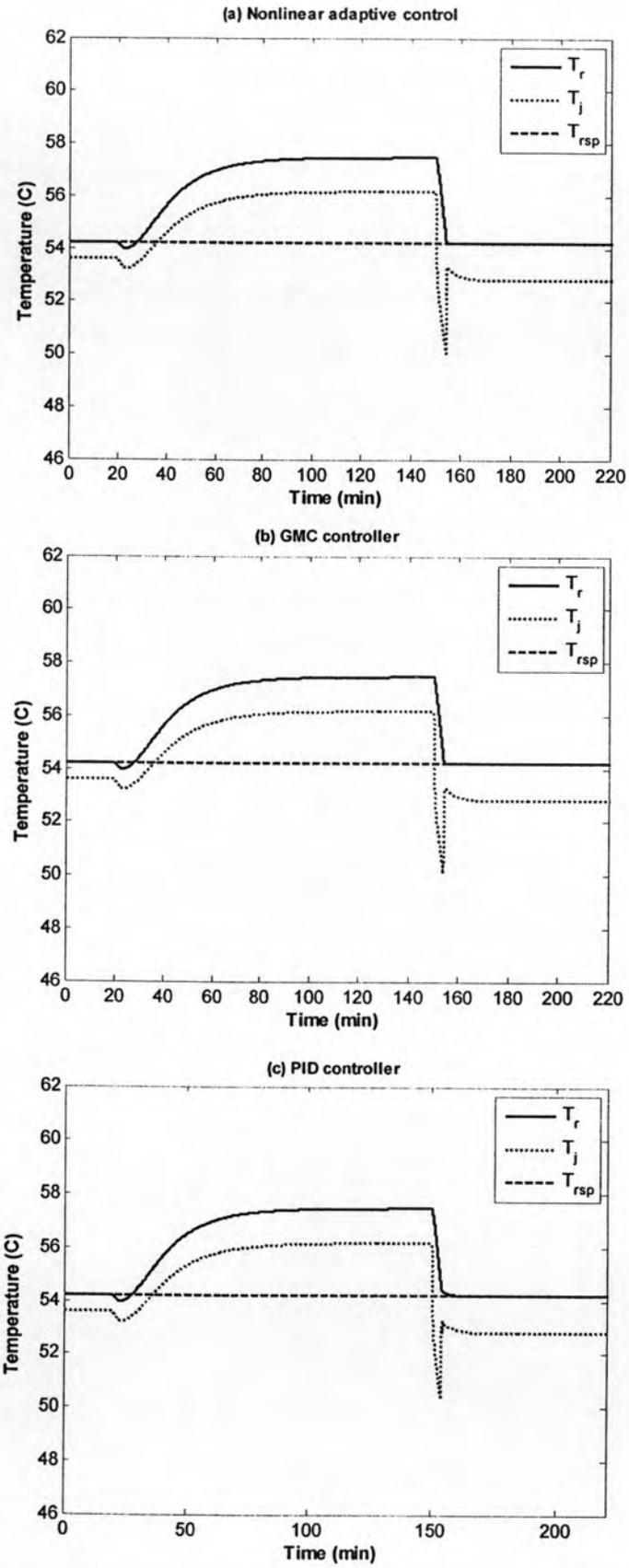

Figure 4.20 The control response of (a) nonlinear adaptive control (b) GMC and (c) PID in plant-mismatch case, -20% k

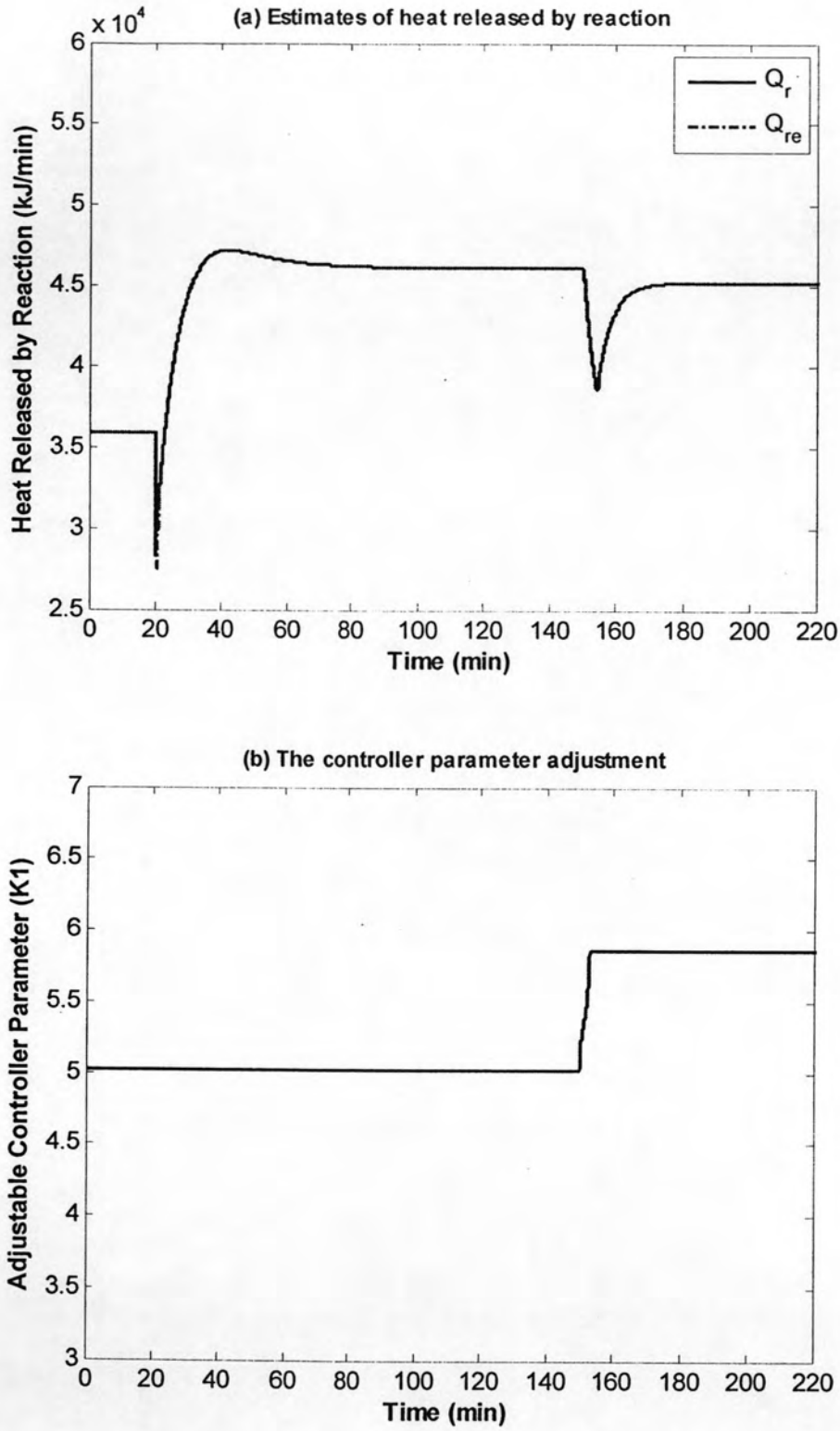

Figure 4.21 (a) Estimates of heat released by reaction and (b) the controller parameter adjustment in plant-mismatch case, -20% *k*